Vector Control Drive of Permanent Magnet Motor without a Shaft Encoder

Eng. Mona F. Moussa*

(Arab Academy for science and technology)
*mona.moussa@yahoo.com

Prof. Yasser Gaber

Prof. Magdy El Attar

Alexandria University

Abstract– Permanent Magnet Synchronous Motors (PMSMs) are receiving increased attention for drive applications because of their high toque to inertia ratio, superior power density, and high efficiency. To control PMSM, position and speed sensors are indispensable because the current should be controlled depending on the rotor position. However, these sensors are undesirable from standpoints of size, cost, maintenance, and reliability. There are different ways of approaching this problem, depending on the flux distribution. This paper presents a novel vector control for a permanent motor drive without use of a shaft sensor. The vector control drive provides a wide range of speeds, high torque capability and high efficiency. Two line-to-line voltages and two stator currents are sensed to produce the stator flux linkage space vector. The angle of this vector is then used to produce the appropriate stator current command signals which can be controlled to maintain zero d-axis current which is the condition of vector control, over a wide range of torque and speed. A speed signals is derived from the rate of change of angle of the flux linkage. Simulation is carried out in order to evaluate the behavior of the proposed method for different operating situations.
The simulation results demonstrate that a good steady-state and transient performances for the proposed sensorless scheme are obtained.

Keywords– Permanent magnet synchronous motor (PMSM), vector control, sensorless control.

List of symbols

R_a	Stator resistance.
L_d, L_q	d-and q-axis inductances.
v_d, v_q	d-and q-axis components of stator voltages.
i_d, i_q	d-and q-axis components of stator currents.
ϕ_d, ϕ_q	d-and q-axis flux linkage.
ω, ω_f	Electrical rotor angular speed and estimated speed.
ϕ_f	Constant flux linkage due to rotor permanent magnet.
P_i, P_o	Input power, and output power.
$\overrightarrow{\Phi_S}, \overrightarrow{e_S}, \overrightarrow{v_S}$	Space vector of stator phase flux linkage, e.m.f, and voltage.
$\overrightarrow{\Phi_L}, \overrightarrow{e_L}, \overrightarrow{v_L}$	Space vector of stator line-to-line stator flux linkage, e.m.f, and voltage.
$\overrightarrow{\iota_S}$	Space vector of line stator current.
i_a, i_b	Stator phase currents.
v_{ab}, v_{bc}	Stator phase voltages.
θ_r, θ_S	Rotor position, and stator position.
$\theta_{\phi L}$	Space angle of the flux-linkage.

I. INTRODUCTION

Improvement of Permanent Magnet (PM) materials is widening the application of PMSMs. Recently, with the advent of high performance (PM) with high coactivity and high residual flux, it has been possible for the PM motors to be superior to general-purpose induction motors in power dentistry, torque-to-inertia ratio, and efficiency. Therefore, the PM motors are of more interest in many industrial applications as substitutes for induction motors. Also, the vector control of PM motors is much simpler than of induction motors because there is no-need to consider the slip frequency as in induction motor drive [1].

However, conventional vector control of PM motor drives requires a motor position sensor to correctly orient the current vector orthogonally to the flux because the rotor flux is obtained from permanent magnets. In such a way, it is possible to directly control the toque by acting simply on the amplitude of the stator current. Thus, we can achieve a high degree of toque control over a wide speed range including the standstill can be achieved [2].

These position sensors or rotational transducers not only increase cost, maintenance, and complexity of the drive, but also impair robustness and reliability of the drive system. Therefore, many researchers have been studying the sensorless drive of the PM motor in view of the robustness, reliability, cost, and so on [1]-[18].

These sensorless techniques can be classified into three categories such as; 1) Position sensing using back e.m.f of the motor. This method can be based on Kalman filtering [3], [4] or state observer [5]-[8]. 2) Position sensing using inductance variation [9]-[13]. 3) Position sensing using flux-linkage variation, which may be based on the measurement of voltages and currents [14]-[17], or on the hypothetical rotor position [18].

In this paper, the proposed sensorless scheme is based on sensing the position via flux-linkage variation. By using motor voltage and currents, synthesis of the flux linkage position signal through which the phase angle of the stator current is controlled. The flux linkage space phasor can be obtained by interesting the back e.m.f which is calculated from measured voltages and currents. This technique represents a simple control system for a PM motor drive with sinusoidal phase current supply, and provides a wide speed range without a shaft encoder.

In [14], the method of position sensing had satisfied the condition of unity power factor operation for PMSM. However, this control strategy in not the optimal in terms of torque production, since the efficiency will not be maximum as the d-axis stator current will not equal zero.

It can be shown that vector control drive corresponds to maximum efficiency maximum and maximum torque per ampere as follows:

The d-q- stator voltage equations of the PMSM in the steady-state operation are expressed as [19]:

$$v_d = R_a\, i_d - \omega\, L_q\, i_q \qquad (1)$$

$$v_q = R_a\, i_q + \omega\, L_d\, i_d + \omega\, \Phi_f \qquad (2)$$

The input power P_i and the developed power P_o are given by:

$$P_i = \frac{3}{2}(v_d i_d + v_q i_q) \tag{3}$$

$$P_o = \frac{3}{2}\omega\left(i_q \Phi_f + (L_d - L_q)i_d i_q\right) \tag{4}$$

And the efficiency $\eta = \frac{P_o}{P_i}$ (5)

The value of current i_d corresponding to maximum efficiency η is obtained from the equation:

$$\frac{\partial \eta}{\partial i_d} = 0 \tag{6}$$

This tends to:

$$i_d = \frac{\omega(L_q - L_d) i_q}{2R_a} \tag{7}$$

For PM motors which have identical rotor structure, the inductance of d-axis equals to that of the q-axis. Substituting $L_d = L_q$ into (6) yields; maximum efficiency takes place when i_d equals zero.

Therefore, in vector control of PMSM, a high dynamic performances without using an excessive current can be achieved if the magnetizing competent i_d of the stator current is maintained at zero, while the torque is controlled using the quadrature component i_q to get optimal type of control and obtain minimum input power and hence, maximum efficiency [20]. That is why, in this paper a novel sensorless drive is based on the vector control scheme of PMSM.

II. PROPOSED SENSORLESS VECTOR CONTROL DRIVE SYSTEM

Recently, many researches are carried out to sensorless control of PMSM vector control drive based on the idea of calculating the rotor position through an estimated angle where the stator voltages and currents signals are used to estimate the instantaneous flux linkage position signal through which the phase angle of the stator current can be controlled to maintain the d-axis current equal to zero over a wide range of torque and speed [17].

A space vector diagram for a PM motor is shown in Fig.1, in which $\overrightarrow{e_S}$ is the line-to neutral e.m.f space vector, and $\overrightarrow{i_S}$ is

Fig. 1 Space vector diagram for sensorless vector controlled PMSM drive.

the phase current vector. The phase flux linkage space vector $\overrightarrow{\Phi_S}$ is obtained by integration of $\overrightarrow{e_S}$. Since the motor normally has no neutral connections, only line voltages are available. The line-to-line e.m.f is denoted as $\overrightarrow{e_L}$, leading $\overrightarrow{e_S}$ by 30^0 in angular space. The line-to-line flux linkage corresponding to $\overrightarrow{e_L}$ is $\overrightarrow{\Phi_L}$.

The e.m.f space vector $\overrightarrow{e_L}$ can be determined from measurements of stator line-to-line voltage v_{ab} and v_{bc} and stator phase current i_a and i_b as follows:

$$\overrightarrow{e_S} = \overrightarrow{v_S} - R_a \overrightarrow{i_S} \tag{7}$$

This equation can be expressed in line values as:

$$\overrightarrow{e_L} = \overrightarrow{v_L} - R_a \overrightarrow{i_L} = \overrightarrow{v_L} - R_a \overrightarrow{i_S}\sqrt{3}\, e^{j\left(\frac{\pi}{6}\right)} \tag{8}$$

The line-to-line stator voltage vector $\overrightarrow{v_L}$ is given by:

$$\overrightarrow{v_L} = \frac{2}{3}\left[v_{ab} + v_{bc}\, e^{j\left(\frac{2\pi}{3}\right)} + v_{ca}\, e^{j\left(\frac{4\pi}{3}\right)}\right] \tag{9}$$

And the line current vector is:

$$\overrightarrow{i_S} = \frac{2}{3}\left[i_a + i_b\, e^{j\left(\frac{2\pi}{3}\right)} + i_c\, e^{j\left(\frac{4\pi}{3}\right)}\right] \tag{10}$$

Substitution of (9) and (10) into (8) yields

$$\overrightarrow{e_L} = e_{LR} + je_{LI} = e_L \lfloor \theta_{\Phi L} + 30° \tag{11}$$

Where, $\overrightarrow{e_{LR}} = v_{ab} - R_a i_a + R_a i_b = v_{ab} + R_a(i_b - i_a)$ (12)

$$\overrightarrow{e_{LI}} = \frac{1}{\sqrt{3}}[v_{ab} + 2v_{bc}] - \sqrt{3}R_a(i_a + i_b) \tag{13}$$

$$\overrightarrow{e_L} = e_L \lfloor \theta_{\Phi L} + 30° \tag{14}$$

The flux linkage space vector $\overrightarrow{\Phi_L}$ is derived from the e.m.f $\overrightarrow{e_L}$ as:

$$\overrightarrow{\Phi_L} = \int \overrightarrow{e_L}\, dt = \Phi_{LR} + j\Phi_{LI} = \phi_L \lfloor \theta_{\Phi L} \tag{15}$$

The real and imaginary components of flux linkage can now be related to the measured quantities by:

$$\Phi_{LR} = \int[v_{ab} - R_a(i_a - i_b)]dt \tag{16}$$

$$\Phi_{LI} = \int \left[\frac{1}{\sqrt{3}}\left(v_{ab} + 2v_{b_c}\right) - \sqrt{3}R_a(i_a + i_b)\right]dt \tag{17}$$

The space angle of the flux linkage is:

$$\theta_{\Phi L} = \tan^{-1}\left(\frac{\Phi_{LI}}{\Phi_{LR}}\right) \tag{18}$$

Since the line-to-line e.m.f $\overrightarrow{e_L}$ is leading the line-to-neutral e.m.f $\overrightarrow{e_S}$ by 30^0 in angular space, and since the line-to-neutral e.m.f $\overrightarrow{e_S}$ is leading the stator phase flux linkage space vector $\overrightarrow{\Phi_S}$ by 90^0, and also $\overrightarrow{e_L}$ is leading $\overrightarrow{\Phi_L}$ by 90^0, then, the stator phase e.m.f $\overrightarrow{e_S}$ should lead the line space vector $\overrightarrow{\Phi_L}$ by 60^0 as should as shown in Fig. 1.

$$\overrightarrow{e_S} = e_{\,S} \lfloor \theta_S \tag{19}$$

$$\theta_S = \theta_{\Phi L} + 60° \tag{20}$$

For vector control, in order to decouple the two components of stator current; namely the flux producing current (i_d) and the torque producing current (i_q), i_d should be zero. Therefore, an independent control of torque and flux is achieved similar to a separately-excited DC motor. Hence,

$$\overrightarrow{i_S^*} = \overrightarrow{i_q^*} \lfloor \theta_r \tag{21}$$

From the above space vector diagram, it is clear that the rotor angle θ_r is lagging the stator angle θ_S by the angle α_v, which is the angle between the d-q frame (rotor frame) and the estimated or e.m.f frame (γ-β frame of $\overrightarrow{e_S}$ and $\overrightarrow{\Phi_S}$).

$$\theta_r = \theta_S - \alpha_v \tag{22}$$

Thus, substituting (22) into (21), the stator current command vector should have the form:

$$\vec{\iota_S^*} = \vec{\iota_q^*} = i_S^* \lfloor \theta_S - \alpha_v \qquad (23)$$

The three phase current commands should then have the instantaneous values:

$$i_a^* = i_S^* \cos(\theta_r)$$
$$i_b^* = i_S^* \cos(\theta_r - 120°) \qquad (24)$$
$$i_c^* = -(i_a^* + i_b^*)$$

Such that, the angle α_v between the line-to-neutral e.m.f $\vec{e_S}$ space vector and the stator current space vector $\vec{\iota_S}$, can be calculated as follows:

$$\alpha_v = \tan^{-1}\left(\frac{\Phi_q}{\Phi_d}\right) \qquad (25)$$

Where, $\Phi_q = L_q i_q^* = L_q i_S^* \qquad (26)$

And, for vector control since $i_d^* = 0$,

$$\Phi_d = \Phi_f \qquad (27)$$

Substituting (26) and (27) into (25) gives:

$$\alpha_v = \tan^{-1}\left(\frac{L_q i_q^*}{\varphi_f}\right) \qquad (28)$$

III. IMPLEMENTATION

Fig. 2 shows a block diagram of the drive system. The system basically has two control loops. In the inner current loop, the two stator terminal voltages and currents are sensed, combined, and integrated first in order to obtain the flux space angle $\theta_{\phi L}°$ (see (16) to (17)). The angle θ_S of the stator phase e.m.f $\vec{e_S}$ space vector is obtained by a 60° shift ahead to $\theta_{\phi L}$ (see (20)). The angle α_v between the vector phase e.m.f $\vec{e_S}$ space vector and the stator current $\vec{\iota_S}$ space vector is calculated (see (28)).
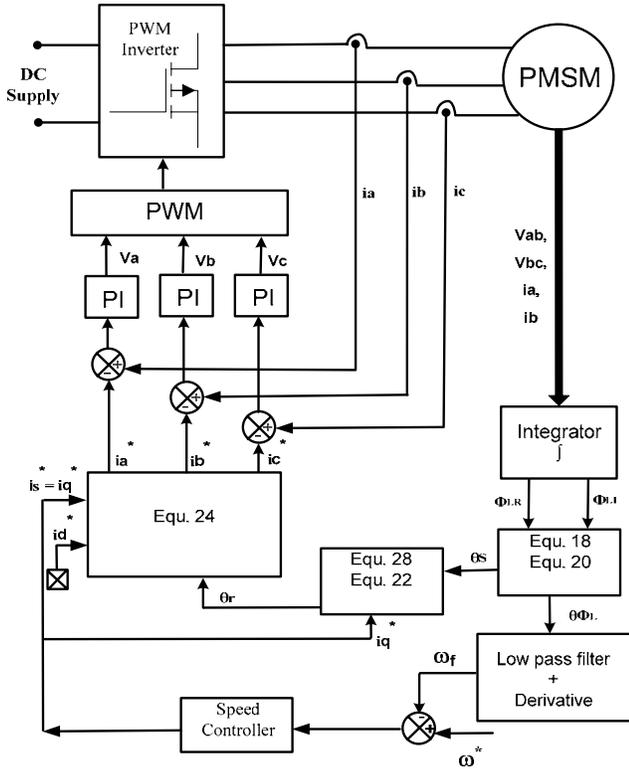
Fig. 2 Block diagram of the sensorless vector controlled PMSM drive system.

Then, the current command angle θ_r is obtained by subtracting the angle θ_s from the calculated angle α_v, (angle between rotor frame and e.m.f frame). Thus, the two cosine functions $\cos(\theta_S-\alpha_v)$ and $\cos(\theta_S-\alpha_v-120°)$ of the two command currents can be generated. Also, the magnitude i_S^* of the two command currents can be obtained from the outer speed loop, such that, the error signal between the command speed signal ω^* and the estimated speed ω_f is implemented to a proportional and integral controller, whose, output is the command q-axis component of current i_q^* which equals to the command stator current i_s^* (see (21)).

Now, the three command currents can be generated (see (24)).

A signal proportional to the motor speed is calculated by the differentiation of the angle $\theta_{\phi L}$

$$\omega_f = \frac{\Delta\theta_{\Phi L}}{\Delta t} \qquad (29)$$

Due to the accuracy and flexibility of the digital signal processor DSP, the above calculations including trigonometric functions, phase shift, differentiation, beside the digital integration can be easily performed. Because $\theta_{\phi L}$ is obtained from an integration of the stator voltages and currents with their high frequency switched waveform resulted from PWM, the differentiation will amplify the high frequency noise in $\theta_{\phi L}$. To eliminate this noise, a low pass filter is required. This is also done in digital form within the DSP.

In implementing this vector control system, the drift of the integrators limits the accuracy of both flux position and speed calculation. That is why; a drift compensation technique like that proposed in [14] may be used to ensure that the average flux linkage with each phase will be zero when the machine operates at steady-state speed and torque. Consequently the calculation errors due to various drift-sources will be effectively reduced.

It is clear from Fig. 3 that, the locus of the flux vector will be a circle in the steady state and will depart only slightly from a circle during a transient since most of the flux linkage arises from the motor magnets.

The maximum and minimum real and imaginary components of the drift can be determined each cycle to give:
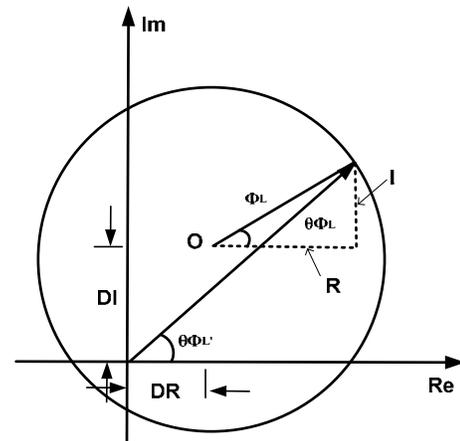

Fig. 3 Locus of the flux linkage vector with drift.

$$DR + jDI = \frac{\phi_{LR(max)} + \phi_{LR(min)}}{2} + j\frac{\phi_{LI(max)} + \phi_{LI(min)}}{2} \quad (30)$$

Then, the calculated angle will become:

$$\theta_{\phi L} = \tan^{-1}\left(\frac{\phi_{LI} - DI}{\phi_{LR} - DR}\right) \quad (31)$$

Therefore, the two components of flux linkage, the real component ϕ_{LR} and the imagining component ϕ_{LI} will appear without any drift or offset.

Near standstill, the e.m.f is too small to be sensed accurately [21], [22]. Thus, an open loop control is necessary to accelerate the motor from standstill to the speed at which the flux linkage angle can be determined. A ''ramp speed command'' starting profile; like that described in [14]; can be applied to provide a smooth start up transient response for the proposed sensorless control scheme, and overcome the starting problem.

It should be noted that, there is a low-frequency limit of control for this vector control sensorless drive, beyond which the stator terminal voltage is dominated by the resistance drop and also the e.m.f residue combined with the inverter noise is inadequate to determine the flux linkage angle. However, several techniques have been proposed to solve this low speed limitation problem [23], [24].

Another limitation of this scheme is its dependence on the parameter sensitivity of the motor such as; the stator resistance by the temperature changes. To solve this disadvantage, parameter identification is proposed in [25].

IV. SIMULATION RESULTS

Simulation of the system has been carried out using Matlab-Simulink, in order to evaluate the behavior of the proposed sensorless vector control drive system.
Fig. 4 shows the transient response of the system due to a step change of the speed command signal from the full load speed 700 rad/sec to 500 rad/sec at time $t_1 = 0.5$ sec, and a step from 500 rad/sec at time $t_2 = 1$ sec to 400 rad/sec, at full load torque (3Nm).

Fig. 5 shows the low frequency performance of the sensorless control system with a step change of the load torque from 3 to 1 Nm at time 1 sec. The simulation results demonstrate that the system can operate adequately at speed = 70 rad/sec (i.e. 10% of the full load speed). The relative error between the actual and estimated speed is equal to zero in steady-state. And the control performance is satisfactory (rapid transient response, small steady state error). Moreover, the estimated position and speed follow exactly the rotor speed and position over a wide range of speed and torque. Therefore, the proposed controlled algorithm has good performance for replacing a shaft sensor over a wide speed range.

To overcome the starting problem, an open-loop control is necessary to accelerate the motor from standstill to the speed at which the flux linkage angle can be reliably determined. Moreover, speed oscillation during the starting process may be minimized by establishing the proper initial rotor angle [22]. One method is to apply a fixed current vector to the motor at standstill and allow its angular oscillation to decay to a predetermined position [14].

Fig. 6 shows the starting performance of the proposed sensorless drive system.
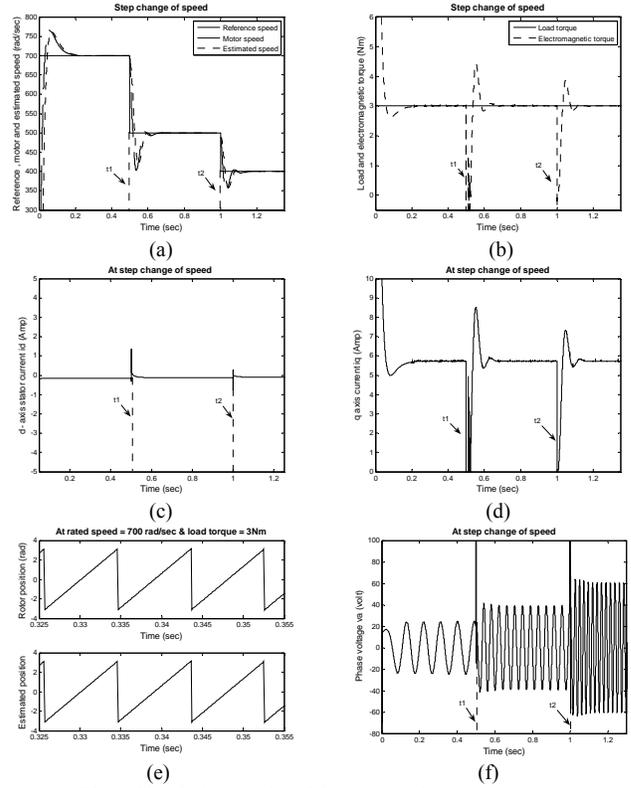

Fig. 4 Simulation results of the proposed sensorless vector controlled drive system.
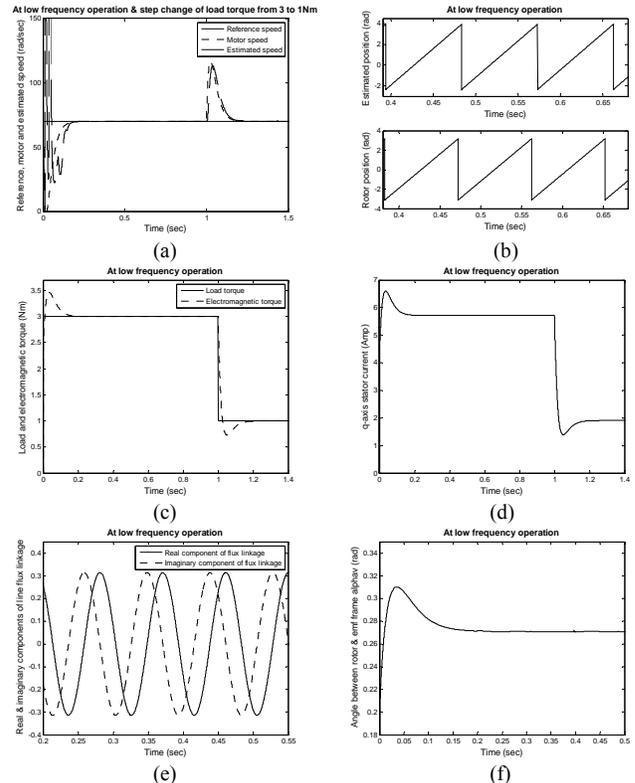

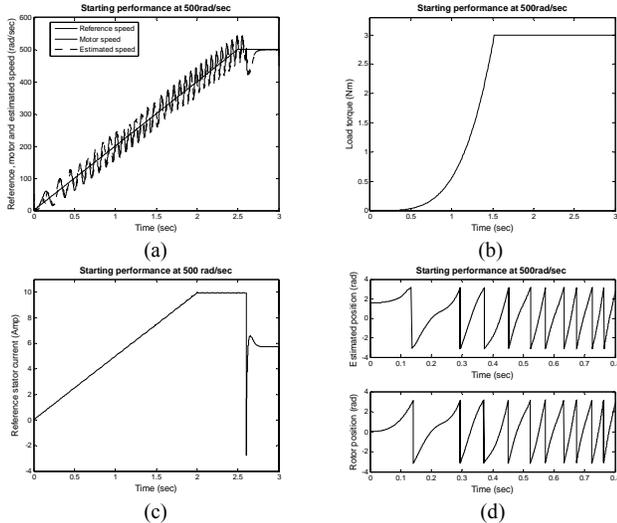Fig. 5 Low frequency performance of the sensorless control system.

Fig. 6 Starting performance of the proposed sensorless drive system.

An open loop control is applied to accelerate the speed from standstill to the speed at which the flux linkage angle $\theta_{\Phi L}$ can be determined.

From the above figures, it is clear that the initial acceleration is limited by the current limit, and the speed response has a small overshoot. Often the problem of a controlled startup is avoided all together the by using open-loop start-up techniques, which provide little control of the torque with unnecessarily high currents.

V. DISCUSSION

The problem of controlling torque, flux, and speed without mechanical sensors in a PMSM drive has been analyzed [26]. Most of these sensorless techniques are based on two basic ideas in the implementation irrelevant on the theory of operation which are:

1- Measuring the rotor position θ_r itself like [18] by using an estimated frame parallel to the original (rotor or d-q frame). This method is usually applied for the conventional decoupled vector control, where $i_d = 0$. In most of these cases, in the current inner loop, there will be a comparison between the actual d and q axis stator currents i_d, i_q and with the command reference d and q-axis i_d* and i_q*. The limitation of this method is its sensitivity to all motor parameters.

2- Measuring the stator angle θ_S itself like [14] by calculating the flux linkage from the currents and voltages. This method has been implemented for unity power factor control drive system, where, in the inner current loop, there will be comparison between the actual phase currents i_a, i_b, i_c with the generated command currents i_a*, i_b*, i_c*. The advantage of this method is its dependence on the stator resistance only. But, it has been proven that the decoupled vector control is better than the unity power factor control since it gives maximum efficiency and maximum torque per ampere current ratio [20].

For this reason, the method presented in this paper will be based on the decoupled vector control by determining the flux linkage angle and the number of the motor parameters which are required will be reduced by one.

VI. SYSTEM DESCRIPTION

Table 1.
3-ϕ Sinusoidal back-EMF PMSM
Rating and Parameters

R_a	2.875Ω
$L_d = L_q$	8.5mH
Φ_f	0.175 V/rad/s
n_{rating}	3000 r.p.m
T_{rating}	3 Nm
J	$0.8*10^{-3}$Kg-m^2
f	0.001Nm/rad/s
Power	1.1 kW
V_{rated}	220 V
frequency	50 Hz

VII. CONCLUSION

The problem of controlling torque, flux, and speed without mechanical sensors in a PMSM drive has been analyzed. Most of these sensorless techniques are based on two basic ideas as follows:

1- Measuring the rotor position θ_r itself like [18] by using an estimated frame parallel to the original (rotor or d-q frame). This method is usually applied for the conventional decoupled vector control, where $i_d = 0$. The limitation of this method is its sensitivity to all motor parameters.

2- Measuring the stator angle θ_S itself like [14] by calculating the flux linkage from the currents and voltages. This method has been implemented for unity power factor control drive system; the advantage of this method is its dependence on the stator resistance only. But, it has been proven that the decoupled vector control is better than the unity power factor control since it gives maximum efficiency and maximum torque per ampere current ratio.

A novel sensorless vector control drive is presented which enables to control motor torque and flux using sufficient and suitable information from the stator voltages and currents to obtain the stator flux angle $\theta_{\phi L}$, which is differentiated to give the estimated speed signal ω_f. Then, the command current angle θ_r which is the difference between the stator angle θ_S and load angle α_v is calculated. This angle is used to enforce the d-axis component of current to be zero. Consequently, the command stator current i_S* is will equal to the q-axis component of current i_q*. Thus, the required decoupling for the two components of stator current is achieved. Hence, a high dynamic performance without using an excessive current can be achieved since the magnetizing component i_d of the stator current is zero, while the torque is controlled using the quadrature component i_q.

The simulation results demonstrate that stator voltage and current signals from a PMSM can be successfully used in a simple vector control system to obtain the necessary position

and speed information for replacing a shaft encoder over a wide speed range. The system works particularly well with a PMSM.

A relatively smooth start can be achieved with open loop using "a ramp acceleration" prior to applying the closed loop control speed. The system is considered to be adequate for the majority of drives that do not require full controlled torque operation down to zero speed.

REFERENCES

[1] Paul P. Acarnley and John F. Wastson, "Review of Position-Sensorless Operation of Brushless Permanent-Magnet Machines," IEEE Trans. Ind. Electron., vol. 53, no. 2, April 2006.

[2] Bon- Ho Bae, IEEE, Seung-Kisal, Jeong-Hyeck Kwon, and Jiseob Beyon, "Implementation of sensorless vector control for super-high-speed PMSM of Turbo -compressor", IEEE Ind. Appl., vol. 39, no. 3, May/June 2003.

[3] Manfred Schroedl, "Sensorless control of permanent magnet synchronous motors," Taylor & Francis, Inc., Washington, DC, vol. 22, pp. 173-185, 1994.

[4] Silverio Bolognani, Luca Tubiana, and Mauro Zigliotto, "EKF-Based sensorless IPM synchronous motor drive for flux-weakening applications", IEEE Trans. Ind. Appl., vol. 39, no. 3, May/June 2003.

[5] Lawrence A. Jones, Jeffrey H. Lang, "A state observer for the permanent-magnet-synchronous Motor," IEEE Trans. Ind. Electron., vol. 36, no. 3, August 1989.

[6] Zhiqian Chen, Muturvo Tomita, Shinji Doki, and Shigeu Okama, "New adaptive sliding observes for position and velocity-sensorless controls of brushless DC motors", IEEE Trans. Ind. Appl., vol. 47, no. 3, June 2000.

[7] Shinji Shinnaka, "New sensorless vector control using minimum order flux state observer in a stationary reference frame for permanent magnet synchronous motors," IEEE, trans. Ind. Electron., vol.53, no.2, April, 2006.

[8] Cristian De Angelo, Guillermo Bossio, Jorge Solsona, and Maria Ines Valla, "A rotor position and speed observer for permanent-magnet motors with nonsinusoidal EMF waveform", IEEE Trans. Ind. Electron., vol. 52, no. 3, June 2005.

[9] Sotahi Ogasawara, and Hiro fumi A kagi, "Implementation and position control performance of a position-sensorless IPM motor drive system based on magnetic saliency," IEEE Trans. Ind. Appl., vol. 34, no. 4, June/August 1998.

[10] Ashok B. Kalkarni, and Mehrdad Ehsani, "A novel position sensor elimination technique for the interior permanent magnet synchronous motor drive", IEEE Trans. Ind. Appl., vol. 28, no. 1, pp.144-150, Jan./Feb. 1992.

[11] Nobuyuki Kasa ,and Hrioshi watanabe, "A mechanical sensorless control system for salient pole Burshless DC motor with Auto

[12] Ji-Hoon Jang, Suing]-Ki Sul, Jung-Ikha and Mitsujiro Sawamura, "Sensorless drive of surface-mounted permanent magnet motor by high-frequency signal injection based on magnetic saliency", IEEE Trans. Ind. Appl., vol. 39, no. 4, July/August 2003.

[13] V. Petrovic, A. M. stankovic, and V. Blasko, "Position estimation in salient PM synchronous motors based on PWM excitation transients", IEEE Trans. Ind. Appl., vol. 39, no. 3, pp. 835-843, May/Jun. 2003.

[14] Rusong Wu, and Gordan R. Selmon, "A Permanent Magnet Motor Drive without a Shaft Sensor," IEEE Trans. Ind. Appl., vol. 27, no. 5, September 1991.

[15] Nesimi Ertigrul and Paul Acarnley, "A new algorithm for sensorless operation of Permanent Magnet Motors," IEEE Trans. Ind. Appl., vol. 30, no.1, January 1994.

[16] T.D. Batzel and K.Y. Lee, "Slotless permanent magnet synchronous motor operation without a high resolution rotor angle sensor", IEEE Trans. Energy Conv., vol. 15, no. 4, pp. 366-371, Dec 2000.

[17] Alfioconsoli, Salvatore Musumeci Angelo Racitic, and Antonia Testa, "Sensorless Vector and Speed Control of Brushless Motor Drives", IEEE Trans. Ind. Electron., vol. 41, no. 1, pp.91-96, February 1994.

[18] Nobuyuki Matsui, "Sensorless PM Brushless DC Motor Drives," IEEE Trans. Ind. Electron., vol. 43,no. 2, April 1996.

[19] P. Pillay and R. Krishnan, "Modeling, Simulation and Analysis of Permanent-Magnet-Motor drives, Part I: The Permanent-Magnet-Motor drive," IEEE Trans. Ind. Appl., vol. 25, no. 2, pp. 265-273, March/April 1989.

[20] Christos Modemlis, and Nikos Margaris, "Loss Minimization in Vector Controlled Interior Permanent-Magnet Synchronous Motor Drives", IEEE Trans. Ind. Electron., vol. 49, no. 6, Nov. /Dec. 2002.

[21] N. Matsui and T. Takeshita, "A novel starting method of sensorless salient-pole brushless motor", IAS Conf. Rec., pp. 386-392, 1995.

[22] Hyunbue Kim, Kum-Kang Hub, Robert D. Loreng, and Thomas M. Jahns, "A novel method for initial rotor position estimation for IPM synchronous machine drives", IEEE Trans. Ind. Appl., vol. 40, no. 5, Sept. 2004.

[23] Joohn-Sheok kim, and seung-kisul, "New approach for the low-speed operation of PMSM drives without rotational position sensors," IEEE Trans. Power Elect., vol. 11, no. 3, May 1996.[

[24] Magnus Janson, Lennart Harnefors, Oskar wallmark, and Mats Leksell, "Synchronization at start up and stable rotation reversal of sensosless nonsalient PMSM drives", IEEE Trans. Ind. Electron., vol. 53, no. 2, April, 2006.

[25] Shinji Ichikawa, Mutuivo Tomita, Shinji Doki & Shigeru Okuma, "Sensorless Control of Permanent Magnet Synchronous Motors Using On-line-Parameter Identification Based on System Identification Theory," IEEE Trans. Ind. Electron., vol. 53, no. 2, April 2006.

[26] Ji-Liang Shi, Tian-Hua Liu, and Yung-Chichang, "Position control of interior permanent magnet synchronous motor without using a shaft position sensor", IEEE Trans. Ind. Electron., vol. 54, no. 4, August 2007.